IEEE Access
Multidisciplinary | Rapid Review | Open Access Journal

SPECIAL SECTION ON INTELLIGENT AND COGNITIVE TECHNIQUES FOR INTERNET OF THINGS

Received September 17, 2019, accepted October 5, 2019, date of publication October 14, 2019, date of current version October 25, 2019.

Digital Object Identifier 10.1109/ACCESS.2019.2947321

Sum Rate Maximization for Multi-User Wireless Powered IoT Network With Non-Linear Energy Harvester: Time and Power Allocation

TIEN-TUNG NGUYEN[1,2], VAN-DINH NGUYEN[3], (Member, IEEE), JONG-HO LEE[4], (Member, IEEE), AND YONG-HWA KIM[1]

[1]Department of Electronic Engineering, Myongji University, Yongin 17058, South Korea
[2]Faculty of Electronics Technology, Industrial University of Ho Chi Minh City, Ho Chi Minh City 700000, Vietnam
[3]Institute of Research and Development, Duy Tan University, Da Nang 550000, Vietnam
[4]School of Electronic Engineering, Soongsil University, Seoul 06978, South Korea

Corresponding author: Yong-Hwa Kim (yongkim@mju.ac.kr)

This work was supported in part by the Korea Electric Power Corporation under Grant R18XA01, and in part by the Basic Science Research Program through the National Research Foundation of Korea (NRF) funded by the Ministry of Science and ICT (NRF-2017R1C1B1012259).

ABSTRACT We consider the ''harvest-then-transmit'' protocol in a wireless powered communication network (WPCN), where an energy-constrained access point (AP) harvests energy from the radio-frequency signals transmitted by a power beacon (PB) for assisting user data transmission. In the wireless information transfer (WIT) phase, AP employs the harvested energy to convey independent signals to multiple users through either time-division multiple access (TDMA) or orthogonal frequency-division multiple access (OFDMA). Aiming to maximize the sum rate (SR) of the WPCN, we jointly optimize the energy harvesting (EH) time and the AP power allocation, considering both the conventional linear and practical nonlinear EH models at the AP. The optimization problems of both TDMA- and OFDMA-enabled WPCNs are formulated as nonconvex programs, which are challenging to solve globally. To achieve an efficient optimal solution to the problem of TDMA-enabled WPCN, we first decompose the original nonconvex problem into three convex subproblems, and then propose a low-complexity iterative algorithm for its solution. For the OFDMA-enabled WPCN, the problem belongs to a difficult class of mixed-integer nonconvex programming due to the involvement of binary variables for subcarrier allocation. To overcome this issue, we convert the problem to a quasi-convex problem and then employ a bisection search to obtain the optimal solution. Simulation results are provided to confirm the benefit of jointly optimizing the EH time and the AP power allocation compared to baseline schemes. The performance of the proposed TDMA-enabled WPCN is shown to be superior to that of the proposed OFDMA-enabled WPCN in terms of SR when the transmit power of PB and the number of antennas of AP are relatively large.

INDEX TERMS Wireless powered communication networks, time-division multiple access, orthogonal frequency-division multiple access, non-linear EH, IoT, nonconvex optimization.

I. INTRODUCTION

Recently, owing to the dramatic development of connected devices, various types of network architectures, such as macrocells, microcells, and picocells, were considered in [1] and have also given rise to Internet-of-Things (IoT) applications. In the IoT networks, several devices and machines are allowed to exchange information through the addition of wireless communication functions [2]–[4]. IoT devices are used to gather information for environmental sensing, smart homes, intelligent transportation, healthcare monitoring, and disaster warnings [5], [6]. Batteries are the most common energy source for IoT devices. However, the periodic replacement or recharging of batteries may not be technically and economically viable underground, in tunnels, toxic environments, in disaster situations, or in the human body [7], [8].

Energy harvesting (EH) technology has received considerable attention to power IoT devices and improve energy

The associate editor coordinating the review of this manuscript and approving it for publication was Min Jia.

This work is licensed under a Creative Commons Attribution 4.0 License. For more information, see http://creativecommons.org/licenses/by/4.0/

efficiency [9]–[19]. IoT devices in wireless networks are powered by harvesting ambient energy such as solar, wind, thermoelectric, and electromechanical [9], [10]. However, EH technologies using natural sources have limitations in specific environments owing to the irregular and unforeseeable nature of ambient sources.

Radio frequency wireless power transfer (RF-WPT) is an EH technology where the nodes of wireless networks collect energy from RF signals and convert this energy into electricity [11]–[19]. For RF-WPT, two cutting-edge EH techniques, have been studied extensively, i.e., simultaneous wireless information and power transfer (SWIPT) [11]–[15], [20] and wireless powered communication network (WPCN) [6], [16]–[19], [21], [22]. For SWIPT, a hybrid access point (HAP) transfers both energy and information to the users simultaneously. The EH receivers in SWIPT-based networks use time switching (TS) and/or power splitting (PS) protocol(s) to harvest energy and signal processing the same signal. For a WPCN, wireless energy transfer (WET) and wireless information transfer (WIT) are completely separate. Unlike SWIPT, energy-constrained devices in a WPCN adopt a ''harvest-then-transmit'' protocol to power from dedicated wireless energy transmitter(s) [6], [16]–[19].

To meet a dramatic growth of demand for wireless data traffic, the sum-rate (SR) or spectral efficiency (SE) maximization will certainly be considered as an important metric and have been widely investigated for resource management due to the trade-off between WET and WIT in WPCNs. A global optimal solution is proposed to maximize the throughput of a WPCN by jointly designing an energy beamforming approach for downlink WET and time allocation for uplink WIT [6]. In a WPCN, the HAP transfers energy to users using WET in the downlink and receives information from users using WIT in the uplink sequentially [16]–[18]. The duration of downlink WET and uplink WIT are optimized using time division multiple access (TDMA) to maximize the throughput [16]. The sum-rate maximization problem of a cognitive radio WPCN is investigated based on joint power control for downlink WET and time allocation among secondary users in uplink WIT [17]. By jointly optimizing subcarrier scheduling and power allocation in the uplink WIT, an iterative algorithm is proposed to maximize the sum-rate of a full duplex orthogonal frequency division multiple access (OFDMA)-based WPCN [18]. In addition, only power beacons (PBs) are used as dedicated wireless energy sources of the energy-constrained devices in downlink WET without communication of the network [6], [19]. The coverage probability has been investigated for a PB-based WPCN [19], where transmitters harvest energy from a PB in WET and then communicate with their corresponding receivers in WIT.

So far, the above existing works [6], [16]–[19] have only focused on downlink WET and uplink WIT in WPCNs. However, some practical scenarios located in toxic environments, underground, tunnels, remote locations, or in disaster areas [23] involve energy-constrained nodes that transmit information to IoT devices under a limited power constraint, and these environments increase the difficulty of replacing batteries or deploying a fixed power supply. Therefore, it is very desirable for the transmitter to harvest energy from the RF signals of a dedicated wireless transmitter to communicate with the IoT devices. Moreover, the energy-constrained node needs to allocate its transmit power for information transmission to serve multiple devices in downlink WIT, which has been not addressed in the previous works.

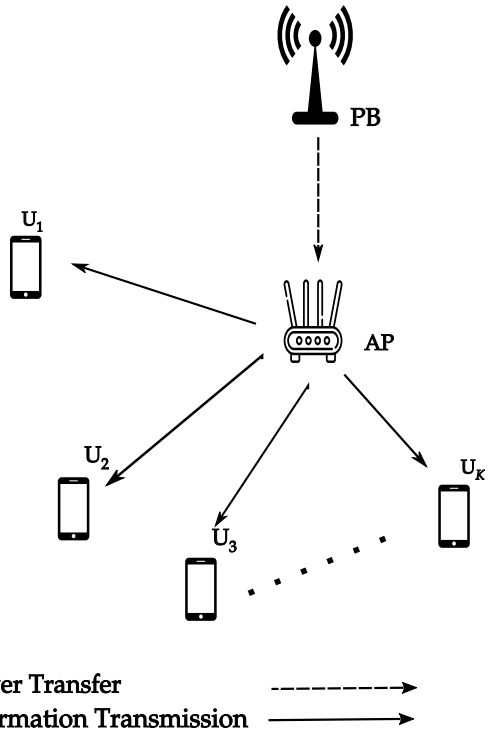

FIGURE 1. System model.

Motivated by the above discussion and literature review, in this paper, we propose a novel PB-based WPCN comprised of one single antenna PB, one energy-constrained multiple-antenna access point (AP), and $K > 1$ single antenna IoT devices, as shown in Figure 1. The AP harvests energy from the RF signals transmitted by the PB to assist the downlink communication between the AP and IoT devices. The goal is to maximize the total SR of the network by jointly optimizing time allocation and transmit power allocation (TPA) at the AP using TDMA and OFDMA.

In short, the major contributions of this paper are summarized as follows:

- We first propose a WPCN in which the AP receives the RF energy from the PB and then delivers information to the IoT devices on the downlink. In the proposed WPCN, AP adopts a ''harvest-then-transmit'' protocol powered by the PB in the WET phase and allocates transmit power to convey information to IoT devices in the WIT phase using TDMA and OFDMA. Contrary to the RF-WPT in [11]–[19], a practical model of EH circuit is taken into account by considering a non-linear EH model with respect to the power received at the AP [24]–[26].

- For TDMA and OFDMA, we formulate the SR maximization problems by jointly optimizing the EH time and transmit power. Both the resulting problems are nonconvex programs, which are troublesome to solve. For TDMA-based problem, toward an efficient solution we first decompose the original nonconvex optimization problem into three convex sub-problems including the EH duration for the AP, time allocation for transferring information from the AP to multiple IoT devices, and TPA for the AP. We then develop a low-complexity iterative algorithm for its solution. For OFDMA-based WPCN, a mixed-integer programming (MIP) problem is transformed into a quasi-convex problem due to the involvement of binary variables for subcarrier allocation, and a bisection search is then employed to obtain the optimal solution.
- Finally, we provide extensive numerical results to confirm that our proposed algorithms are efficient in terms of the SR. In particular, we compare the SR of the proposed method with that of baseline schemes, i.e., a fixed EH time [14], [15] and equal time allocation (ETA) [16], [17]. In addition, simulation results also reveal that the TDMA-enabled WPCN outperforms the OFDMA-enabled WPCN when the transmit power of the PB and the number of AP's antennas are relatively large.

This paper is organized as follows. Section II presents the system model, energy harvesting model and problem formulations for TDMA and OFDMA. Section III and IV investigate the SR maximization problems for the proposed TDMA-enabled WPCN and OFDMA-enabled WPCN, respectively. In Section V, the numerical results are presented in order to demonstrate the effectiveness of the proposed solutions. Finally, Section VI concludes this paper.

II. DESCRIPTION OF THE SYSTEM MODEL AND ENERGY HARVESTING MODEL

In this section, we first describe the system model with multiple IoT users and introduce the EH model with conventional linear and the practical non-linear energy harvesters. Then, the SR maximization problems for TDMA-enabled and OFDMA-enabled WCPN are formulated.

A. SYSTEM MODEL

As shown in Figure 1, we consider a WPCN consisting of one single-antenna power beacon PB and one energy-constrained AP equipped with N_T antennas, and $K > 1$ single-antenna IoT users. A total transmission time block, denoted by T_{max}, is divided into two phases such as the WET phase from the PB to AP and the WIT phase from the AP to IoT users. Without loss of generality, T_{max} is normalized to one, i.e., $T_{max} = 1$. The frameworks for the TDMA- and OFDMA-enabled schemes are depicted in Figure 2(a) and 2(b), respectively. It is assumed that channel state informations (CSIs) are perfectly known at the AP and by all users [16], [27].

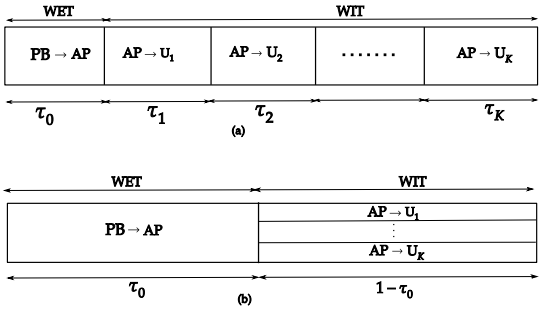

FIGURE 2. (a) Frame structure of TDMA-enabled WPCN. (b) Frame structure of OFDMA-enabled WPCN.

B. ENERGY HARVESTING MODEL

In IoT networks, all transceivers including AP should be low-cost and low-power devices equipped with very limited battery capacity. As a result, it is of practical interest to adopt the "harvest-then-transmit" protocol [16] at the energy-constrained AP to harvest energy from the PB during the WET phase and then convey information to K users during the WIT phase. Let $\tau_0 \in (0, 1)$ be the time fraction spent during WET. The total power received at the AP is $P_{Ein} = \mathrm{P_B}\|\mathbf{h}_p\|^2$, where $\mathrm{P_B}$ is the transmit power at the PB, $\mathbf{h}_p \in \mathbb{C}^{N_T \times 1}$ is the channel vector from the PB to AP. In this study, we consider two EH models as follows:

• Traditional EH model: The amount of harvested energy at the AP [27] can be given by

$$E_{\mathrm{ln}} = \eta P_{Ein} \tau_0, \tag{1}$$

where $\eta \in (0, 1]$, is the constant energy conversion efficiency of the AP.

• Practical non-linear EH model: However, in practice, owing to the limitation of EH circuits, the harvested energy at the AP is non-linear. In this study, we use a non-linear RF EH model [24]–[26]; then, the harvested energy at the AP is given as

$$E_{\mathrm{nln}} = \left(\frac{\psi - M\pi}{1 - \pi}\right)\tau_0, \tag{2}$$

$$\pi = \frac{1}{1 + \exp(ab)}, \tag{3}$$

$$\psi = \frac{M}{1 + \exp(-a(P_{Ein} - b))}, \tag{4}$$

where the constant parameters M, a, b depend on characteristics of the EH circuits [24]–[26].

C. TDMA-ENABLED WPCN

As illustrated in Figure 2 (a), the AP uses energy harvested from the first phase to consecutively transmit signals to K IoT users during the WIT phase in the remaining $1 - \tau_0$ time fraction at the same frequency band, B, by using TDMA tranmisison. For simplicity, the maximum ratio transmission (MRT) technique is used to beamform the signal users [27]. The transmit power of the AP allocated for information transmission to the k-th user during τ_k is denoted by p_k. The channel vector from the AP to k^{th} user is denoted as $\mathbf{g}_k \in \mathbb{C}^{N_T \times 1}$.

Hence, the achievable rate of user-k is given as

$$r_k^{\text{TDMA}} = B\tau_k \log\left(1 + p_k \bar{\gamma}_k\right), \tag{5}$$

where $\bar{\gamma}_k = \frac{\|\mathbf{g}_k\|^2}{B\delta^2}$ with δ^2 being the noise spectral density. As a result, the total SR of the TDMA-enabled WPCN is given as

$$\begin{aligned} R_{sum}^{\text{TDMA}} &= \sum_{k=1}^{K} r_k^{\text{TDMA}} \\ &= \sum_{k=1}^{K} B\tau_k \log\left(1 + p_k \bar{\gamma}_k\right). \end{aligned} \tag{6}$$

Our goal is to maximize the total SR of K IoT users subject to the time fraction and power constraints. By jointly optimizing τ_0 and p_k, the optimization problem of interest is stated as follows:

$$\begin{aligned} (\text{P1}): \max_{\tau_0, \{\tau_k\}, \{p_k\}} \; & R_{sum}^{\text{TDMA}} \\ \text{s.t. C1}: \; & 0 < \tau_k \leq 1, \quad \forall k \in \mathcal{K} \triangleq \{1, \ldots, K\}, \\ \text{C2}: \; & \sum_{k=0}^{K} \tau_k \leq 1, \quad \forall k \in \mathcal{K}, \\ \text{C3}: \; & p_k \geq 0, \quad \forall k \in \mathcal{K}, \\ \text{C4}: \; & \sum_{k=1}^{K} \tau_k p_k \leq E_\Theta \tau_0, \quad \forall k \in \mathcal{K}, \end{aligned} \tag{7}$$

where C4 implies that the total energy consumed by the AP in the WIT phase should be less than the harvested energy in the WET phase, and

$$E_\Theta = \begin{cases} \eta P_{Ein}, & \text{linear EH model} \\ \left(\dfrac{\psi - M\pi}{1 - \pi}\right), & \text{non-linear EH model.} \end{cases} \tag{8}$$

The objective of (P1) is a non-concave function in p_k and τ_k. In addition, the coupling between τ_k and p_k in the left-hand side of C4 results in a nonconvex constraint. Thus, (P1) is a non-convex problem and thus it cannot be solved directly. A detailed optimal solution, which provides more insight into the structure of the optimal solution, for this problem will be presented in Section III.

D. OFDMA-ENABLED WPCN

For benchmarking purpose, we also consider the OFDMA-enabled WPCN. As shown in Figure 2(b), the AP transmits data to the users by using OFDMA over N orthogonal subcarriers (SCs) in the same duration $(1 - \tau_0)$ of the WIT phase. To eliminate interference, each SC is allocated to each user. We introduce a binary SC assignment variable $x_{k,n}$, $x_{k,n} = 1$ if the SC n is allocated to the k-th user for the WIT phase; otherwise, $x_{k,n} = 0$. The channel power gain of the link from the AP to the k-th user on the SC n is denoted as $\mathbf{g}_{k,n} \in \mathbb{C}^{N_T \times 1}$. The transmit power of the AP assigned on the SC n for information transmission to the k-th user is denoted as $p_{k,n}$. Therefore, the achievable rate of the k-th user on the n-th SC is given as

$$r_{k,n}^{\text{OFDMA}} = \frac{B\left(1 - \tau_0\right)}{N} x_{k,n} \log\left(1 + p_{k,n} \bar{u}_{k,n}\right), \tag{9}$$

where $\bar{u}_{k,n} = \frac{\|\mathbf{g}_{k,n}\|^2}{(B/N)\delta^2}$.

Then, the total SR of the OFDMA-enabled WPCN scheme is calculated as

$$\begin{aligned} R_{sum}^{\text{OFDMA}} &= \sum_{k=1}^{K} \sum_{n=1}^{N} r_k^{\text{OFDMA}} \\ &= \sum_{k=1}^{K} \sum_{n=1}^{N} \frac{B\left(1 - \tau_0\right)}{N} x_{k,n} \log\left(1 + p_{k,n} \bar{u}_{k,n}\right). \end{aligned} \tag{10}$$

By jointly optimizing $\tau_0, x_{k,n}, p_{k,n}$, the optimization problem for the OFDMA-enabled WPCN can be mathematically formulated as

$$\begin{aligned} (\text{P2}): \max_{\tau_0, \{p_{k,n}\}, \{x_{k,n}\}} \; & R_{sum}^{\text{OFDMA}} \\ \text{s.t. C1}: \; & p_{k,n} \geq 0, \quad \forall k \in \mathcal{K}, \; \forall n \in \mathcal{N} \triangleq \{1, \ldots, N\}, \\ \text{C2}: \; & \sum_{k=1}^{K} x_{k,n} = 1, \quad \forall k \in \mathcal{K}, \; \forall n \in \mathcal{N}, \\ \text{C3}: \; & x_{k,n} \in \{0, 1\}, \quad \forall k \in \mathcal{K}, \; \forall n \in \mathcal{N}, \\ \text{C4}: \; & (1 - \tau_0) \sum_{k=1}^{K} \sum_{n=1}^{N} x_{k,n} p_{k,n} \leq E_\Theta \tau_0, \\ & \qquad \forall k \in \mathcal{K}, \; \forall n \in \mathcal{N}, \\ \text{C5}: \; & 0 < \tau_0 \leq 1. \end{aligned} \tag{11}$$

Constraints C2 and C3 indicate that one SC is assigned exactly to each link. Constraint C4 implies that the total energy consumed by the AP in the WIT phase should be less than the harvested energy in the WET phase.

We can see that the strong coupling between τ_0, $p_{k,n}$ and $x_{k,n}$ in problem (P2) results in the non-concavity of its objective and nonconvexity of C4. Moreover, (P2) belongs to the class of a mixed-integer nonconvex programming (MINP) due to the presence of the binary assignment variable $x_{k,n}$. Note that for any $K > 1$, the objective and constraints of both optimization problems are essentially different. The main difficulty of solving (P1) is due to the strong coupling between $\{\tau_k\}$ and $\{p_k\}$, while that of (P2) is due to the presence of binary decision variables. Although finding an optimal solution to (P2) is more challenging than (P1), the developments of the former cannot be reused to devise an optimal solution for the later due to the different structure of problem designs and different set of optimization variables (i.e., see **Algorithms 1** and **2** presented shortly in Section III and Section IV, respectively). Nevertheless, an effective method to find the optimal solution for (P2) will be given in Section IV.

III. JOINT ENERGY HARVESTING TIME AND POWER ALLOCATION FOR TDMA-ENABLED WPCN

In this section, we propose an effective method to determine SR maximization introduced as in (P1).

First, we let $p_k = \frac{E_k}{\tau_k}$, and rewrite (P1) as

$$\begin{aligned}(\text{P1-1}): \max_{\tau_0,\{\tau_k\},\{E_k\}} & \sum_{k=1}^{K} B\tau_k \log\left(1+\frac{E_k}{\tau_k}\bar{\gamma}_k\right)\\ \text{s.t. C1}: & \ 0<\tau_k\le 1, \quad \forall k\in\mathcal{K},\\ \text{C2}: & \sum_{k=0}^{K}\tau_k \le 1, \quad \forall k\in\mathcal{K},\\ \bar{\text{C}}_3: & \sum_{k=1}^{K} E_k \le E_\Theta \tau_0,\\ \bar{\text{C}}_4: & \ E_k \ge 0, \quad \forall k\in\mathcal{K}. \end{aligned} \tag{12}$$

Each function in the objective of (P1-1) has the form of $x\log(1+y/x)$ which is jointly concave in x and y [6]. In addition, all constraints are linear. Hence, (P1-1) is still a convex optimization problem. To solve this problem, we introduce a distributed method that has two main steps. In **step 1**, we first optimize τ_k, $1 \le k \le K$, with given E_k and τ_0. In **step 2**, the optimal solution to E_k is found by a bisection search with the given the optimized τ_k^* and the EH time τ_0. Finally, we determine the optimal τ_0^* using a golden section search. The overall process of determining the optimal solution to (P1) is summarized in **Algorithm 1**.

Step 1: With given E_k and τ_0, we reformulate (P1-1) as

$$\begin{aligned}(\text{P1-2}): \max_{\{\tau_k\}} & \sum_{k=1}^{K} B\tau_k \log_2\left(1+\frac{E_k}{\tau_k}\bar{\gamma}_k\right)\\ \text{s.t., C1}: & \ 0<\tau_k\le 1, \quad \forall k\in\mathcal{K},\\ \bar{\text{C}}_2: & \sum_{k=1}^{K}\tau_k \le 1-\tau_0, \quad \forall k\in\mathcal{K}. \end{aligned} \tag{13}$$

The optimal information transmission duration τ_k^* for each user is found by the following proposition.

Proposition 1: With a given E_k and τ_0, the optimal τ_k^* can be expressed by

$$\tau_k^* = \frac{(1-\tau_0)E_k\bar{\gamma}_k}{\sum_{k=1}^{K} E_k\bar{\gamma}_k}, \quad 1\le k\le K. \tag{14}$$

Proof: See Appendix A.

Step 2: By substituting τ_k^* into the objective of (P1-2), we can obtain

$$\begin{aligned}(\text{P1-3}): \max_{\tau_0,\{E_k\}} & \ B(1-\tau_0)\log\left(1+\frac{\sum_{k=1}^{K} E_k\bar{\gamma}_k}{1-\tau_0}\right)\\ \text{s.t. C1}: & \ 0\le\tau_0\le 1,\\ \bar{\text{C}}_3: & \sum_{k=1}^{K} E_k \le E_\Theta\tau_0,\\ \bar{\text{C}}_4: & \ 0\le E_k, \quad \forall k\in\mathcal{K}. \end{aligned} \tag{15}$$

As the objective function of (P1-3) is concave on both variables τ_0 and $\{E_k\}$ and all constraints of (P1-3) are linear. Therefore, the problem in (P1-3) is easily verified to be a jointly concave problem. To address (P1-3), we first fix the EH duration τ_0 to $\bar{\tau}$; then, (P1-3) is expressed as

$$\begin{aligned}(\text{P1-4}): \ \mathfrak{A}(\bar{\tau}) \triangleq \max_{\{E_k\}} & B(1-\bar{\tau})\log\left(1+\frac{\sum_{k=1}^{K} E_k\bar{\gamma}_k}{1-\bar{\tau}}\right)\\ \text{s.t. } \tilde{\text{C}}_3: & \sum_{k=1}^{K} E_k \le E_\Theta\bar{\tau},\\ \bar{\text{C}}_4: & \ 0\le E_k, \quad \forall k\in\mathcal{K}. \end{aligned} \tag{16}$$

The optimal energy allocation $\{E_k^*\}$ is obtained based on the following proposition.

Proposition 2: With a given $\bar{\tau}$, the optimal E_k^* is achieved

$$E_k^* = (1-\bar{\tau})\left[\frac{B}{\chi}-\frac{\Xi}{\bar{\gamma}_k}\right]^+, \tag{17}$$

where $x^+ \triangleq \max(x,0)$ and $\Xi = \sum_{i=1,i\ne k}^{K} E_i\left(\frac{\bar{\gamma}_i}{1-\bar{\tau}}\right)+1$.

Proof: See Appendix B.

To determine the optimal E_k^*, we use a bisection search for the dual variable χ between $\underline{\chi}=0$ and a sufficiently large $\bar{\chi}$ with given $\tau_0=\bar{\tau}$. The complexity of the bisection search used for determing the optimal E_k^* is $O\left(\log_2\left(\frac{1}{\varsigma}\right)\right)$, where ς represents the search accuracy. Our remaining task is to determine the optimal EH τ_0 to obtain the maximum SR by calculating $\tau_0^* = \arg\max_{0<\tau_0<1}\mathfrak{A}(\tau_0)$. We note that the objective function $\mathfrak{A}(\tau_0)$ is concave on τ_0, thus, we can utilize the golden section search to obtain the optimal τ_0^*. For unimodal functions, the golden section search method always guarantees convergence to the global point [28]. Hence, the global optimality for finding τ_0^* from **Algorithm 1** is also satisfied.

IV. JOINT ENERGY HARVESTING TIME, SUBCARRIER ALLOCATION AND POWER ALLOCATION FOR OFDMA-ENABLED WPCN

In this section, we present the joint EH time, SC and power allocation solution to maximize the SR for the OFDMA-enabled WPCN. Inspired by the approach in [15], we propose a method to solve this problem. First, we aim to simplify the problem by rewriting C4 in (P2) as

$$\tau_0 \ge \frac{\sum_{k=1}^{K}\sum_{n=1}^{N} x_{k,n}p_{k,n}}{\sum_{k=1}^{K}\sum_{n=1}^{N} x_{k,n}p_{k,n}+E_\Theta} \tag{18}$$

The objective of (P2) is a non-increasing function with respect to τ_0. Thus, from constraint C4 in (P2), the optimal

Algorithm 1 Proposed Algorithm to Solve Problem (P1)

1: **Initialize:** $\tau_{\min}=0, \tau_{\max}=1$, step $\mho=\left(\sqrt{5}-1\right)/2$ [28], φ is a small value for the stopping criterion.
2: **Repeat:**
3: Calculating $\tau_1=\tau_{\max}-(\tau_{\max}-\tau_{\min})\,\mho$ and $\tau_2=\tau_{\min}+(\tau_{\max}-\tau_{\min})\,\mho$.
4: Obtaining $\mathbf{E}^*$as in (17) by the bisection search over χ with given τ_1.
5: Obtaining $z(\tau_1)=B(1-\tau_1)\log\left(1+\frac{\sum_{k=1}^{K}E_k^*\bar{\gamma}_k}{1-\tau_1}\right)$.
6: Obtaining $\mathbf{E}^*$as in (17) by the bisection search over χ with given τ_2.
7: Obtaining $z(\tau_2)=B(1-\tau_2)\log\left(1+\frac{\sum_{k=1}^{K}E_k^*\bar{\gamma}_k}{1-\tau_2}\right)$.
8: If $z(\tau_1)>z(\tau_2)$
9: $\tau_{\max}=\tau_2$
10: Esle
11: $\tau_{\min}=\tau_1$.
12: **Until**: $|\tau_{\max}-\tau_{\min}|<\varphi$
13: **Output:**
14: Finding the optimal $\tau_0^*=(\tau_{\max}+\tau_{\min})/2$.
15: Obtaining $\mathbf{E}^*$as in (17) by the bisection search over χ with given τ_0.
16: Finding the optimal τ_k^* based on (14).
17: Finding the optimal $p_k^*=E_k^*/\tau_k^*$.

τ_0 should be hold for a given power allocation

$$\tau_0=\frac{\sum_{k=1}^{K}\sum_{n=1}^{N}x_{k,n}p_{k,n}}{\sum_{k=1}^{K}\sum_{n=1}^{N}x_{k,n}p_{k,n}+E_\Theta}. \tag{19}$$

By substituting (19) into (10), we obtain

$$\bar{R}_{sum}^{\text{OFDMA}}=\frac{BE_\Theta}{N\Phi}\sum_{k=1}^{K}\sum_{n=1}^{N}x_{k,n}\log\left(1+p_{k,n}\bar{u}_{k,n}\right), \tag{20}$$

where $\Phi=\sum_{k=1}^{K}\sum_{n=1}^{N}x_{k,n}p_{k,n}+E_\Theta$.
Then, (P2) can be rewritten as

$$\begin{aligned}(\text{P2-1}):\ &\max_{\mathbf{p},\mathbf{x}}\bar{R}_{sum}^{\text{OFDMA}}\\ &\text{s.t. C1:}p_{k,n}\geq 0,\quad \forall k\in\mathcal{K},\ \forall n\in\mathcal{N},\\ &\quad\text{C2:}\sum_{k=1}^{K}x_{k,n}=1,\quad \forall n\in\mathcal{N},\\ &\quad\text{C3:}x_{k,n}\in\{0,1\},\quad \forall k\in\mathcal{K},\ \forall n\in\mathcal{N},\end{aligned} \tag{21}$$

where $\mathbf{p}=\{p_{k,n},\forall k,\forall n\}$ and $\mathbf{x}=\{x_{k,n},\forall k,\forall n\}$.

Lemma 1: Suppose that g is a twice differentiable function. When $ax+b>0$, $g(x)/(ax+b)$ is quasiconvex if $y=g(x)$ is convex, $g(x)/(ax+b)$ is quasi-concave if $y=g(x)$ is concave.

Proof: The detailed proof can be found in [29] and thus omitted her for brevity.

Based on *Lemma 1*, we can observe that the objective of (P2-1) is a quasi-concave function of $p_{k,n}$ with a given SC $\mathbf{x}$. To solve (P2-1), we now use the quasi-convex method by introducing a slack variable θ as an upper bound of the problem [14]. Then, (P2-1) can be rewritten as

$$\begin{aligned}(\text{P2-2}):\ &\min\theta\\ &\text{s.t.}\left[\max_{\mathbf{x},\mathbf{p}}\bar{R}_{sum}^{\text{OFDMA}}\leq\theta,\ \text{s.t. C1,C2,C3}\right].\end{aligned} \tag{22}$$

This holds because minimizing θ means determining the least upper bound of the objective function of (P2-1) while the maximum value of the objective function in (P2-1) is equal to this least upper bound. Thus, (P2-2) can be further expressed as

$$\begin{aligned}(\text{P2-3}):\ &\min_{\theta\geq 0}\theta\\ &\text{s.t.}\left[\min_{\mathbf{x},\mathbf{p}}F(\mathbf{x},\mathbf{p},\theta)\geq 0\ \text{s.t. C1,C2,C3}\right],\end{aligned} \tag{23}$$

where

$$\begin{aligned}F(\mathbf{p},\mathbf{x},\theta)=\theta&\left(\sum_{k=1}^{K}\sum_{n=1}^{N}x_{k,n}p_{k,n}+E_\Theta\right)\\ &-\frac{BE_\Theta}{N}\sum_{k=1}^{K}\sum_{n=1}^{N}x_{k,n}\log\left(1+p_{k,n}\bar{u}_{k,n}\right).\end{aligned} \tag{24}$$

If the problem

$$\min_{\mathbf{x},\mathbf{p}}F(\mathbf{x},\mathbf{p},\theta)\geq 0\ \text{s.t. C1,C2,C3} \tag{25}$$

has a non-negative optimal value, θ will become a true upper bound of the objective function in (P2-1). Therefore, to find the solution for the problem in (P2-1), we first solve (P2-3) with a given θ and then using bisection search over θ. From (24), we can reformulate $F(\mathbf{p},\mathbf{x},\theta)$ as

$$F(\mathbf{p},\mathbf{x},\theta)=\sum_{k=1}^{K}\sum_{n=1}^{N}x_{k,n}F_{k,n}\left(p_{k,n},\theta\right)+\theta E_\Theta, \tag{26}$$

where $F_{k,n}\left(p_{k,n},\theta\right)=\theta p_{k,n}-\frac{BE_\Theta}{N}\log\left(1+p_{k,n}\bar{u}_{k,n}\right)$.

For a given SC allocation $\mathbf{x}$, the optimal power allocation of the problem in (25) over the SC with $x_{k,n}=1$ can be solved by addressing the following sub-problems:

$$\min_{p_{k,n}\geq 0}F_{k,n}\left(p_{k,n},\theta\right) \tag{27}$$

It can be seen that $\log\left(1+p_{k,n}\bar{u}_{k,n}\right)$ is a concave function in $p_{k,n}$, leading to a convexity of the objective in (27); thus, by setting the derivative $\frac{\partial F_{k,n}(p_{k,n},\theta)}{\partial p_{k,n}}$ to zero, we obtain

$$\frac{\partial F_{k,n}\left(p_{k,n},\theta\right)}{\partial p_{k,n}}=\theta-\frac{BE_\Theta}{N}\left(\frac{\bar{u}_{k,n}}{1+p_{k,n}\bar{u}_{k,n}}\right)=0. \tag{28}$$

Solving the equation in (28), we have

$$p_{k,n}^{*}=\left[\frac{BE_{\Theta}}{\theta N}-\frac{1}{\bar{u}_{k,n}}\right]^{+}. \tag{29}$$

By substituting (29) into (24), we obtain

$$F_1\left(\mathbf{x},\theta\right)=\sum_{k=1}^{K}\sum_{n=1}^{N}x_{k,n}Q_{k,n}\left(\theta\right)+\theta E_{\Theta}, \tag{30}$$

where

$$Q_{k,n}\left(\theta\right)=\left[\frac{BE_{\Theta}}{N}-\frac{\theta}{\bar{u}_{k,n}}\right]^{+} -\frac{BE_{\Theta}}{N}\log\left(1+\left[\frac{BE_{\Theta}}{\theta N}\bar{u}_{k,n}-1\right]^{+}\right). \tag{31}$$

Thus, the problem in (25) becomes

$$\begin{aligned}&\min_{\mathbf{x}} F\left(\mathbf{x},\theta\right)\\ &\text{s.t. C2}:\sum_{k=1}^{K}x_{k,n}=1,\quad \forall k\in\mathcal{K},\ \forall n\in\mathcal{N},\\ &\text{C3}: x_{k,n}\in\{0,1\},\quad \forall k\in\mathcal{K},\ \forall n\in\mathcal{N}.\end{aligned} \tag{32}$$

Clearly, $Q_{k,n}\left(\theta\right)$ is independent of variable $x_{k,n}$. Thus, the optimal $x_{k,n}^{*}$ for problem (32) can be easily found as

$$x_{k^{*},n}^{*}=\begin{cases}1, & k=k^{*}\\ 0, & \forall k\neq k^{*},\end{cases} \tag{33}$$

where

$$k^{*}=\arg\min_{k} Q_{k,n}\left(\theta\right). \tag{34}$$

Note that $F\left(\mathbf{p},\mathbf{x},\theta\right)$ in (26) is a monotonously increasing function with respect to θ. Thus, we can use a bisection search over θ to determine the optimal θ^{*}. In general, a solution to (P2) is summaried in **Algorithm 2**, where $\theta_l=0, \theta_u=\Delta$ and ε are denoted as the lower and upper bound of the bisection search over θ, the predefined accuracy of bisection search, respectively. The upper bound Δ is obtained as

$$\Delta=BK\log\left(1+E_{\Theta}\max_{k,n}\left\{\bar{u}_{k,n}\right\}\right). \tag{35}$$

For the bisection search, the computational complexity is similar to $O\left(\log_2\left(\varepsilon^{-1}\right)\right)$. The complexity of the golden section search is $O\left(\log_2\left(\varsigma^{-1}\right)\right)$. The complexity for SC allocation and power allocation corresponding to step 3 and step 4 in **Algorithm 2** is $O\left(N+NK\right)$ [15]. Thus, the general computational complexity of our proposed algorithm for the TDMA-enabled WPCN and the OFDMA-enabled WPCN are $O\left(\log_2\left(\varepsilon^{-1}\right)\log_2\left(\varsigma^{-1}\right)\right)$ and $O\left(\log_2\left(\varepsilon^{-1}\right)\left(N+NK\right)\right)$, respectively.

Algorithm 2 Proposed Algorithm to Solve Problem (P2)

1: **Initialize**: $\theta_l=0, \theta_u=\Delta, m=0$; ε is a small value for the stopping criterion.
2: **Repeat:** $\theta(m)=\left(\theta_l+\theta_u\right)/2$;
3: Obtaining optimal $p_{k,n}^{*}$ based on (29);
4: Obtaining optimal $\mathbf{x}^{*}$ based on (33);
5: Let $\mathbf{x}(m)=\mathbf{x}^{*}$ and $\mathbf{p}(m)=\mathbf{p}^{*}$;
6: **If** $F\left(\mathbf{p}(m),\mathbf{x}(m),\theta(m)\right)>0$,
7: $\theta_u=\theta(m)$;
8: **Else**
9: $\theta_l=\theta(m)$;
10: **End**
11: $m=m+1$;
12: **Until** $\theta_u-\theta_l<\varepsilon$;
13: **Output:**
14: Optimal power allocation: $\mathbf{p}^{*}=\mathbf{p}^{*}(m)$;
15: Optimal subcarrier allocation: $\mathbf{x}^{*}=\mathbf{x}(m)$;

TABLE 1. Simulation parameters.

Parameter	Value
System bandwidth, B	180 kHz [31]
Number of subcarriers	12 [31]
Noise spectral density, δ^2	-117 dBm/Hz
Energy conversion efficiency, η	0.8 [27]
M	24 mW [26]
a	0.014 [26]
b	150 [26]

V. SIMULATION RESULTS

In the simulations, all the channels are assumed to be experiencing a Rayleigh fading, and channel gains are modeled as $10^{-3}\vartheta^2 d^{-\alpha}$ [30], where d represents the link distance and ϑ^2 is the exponential distribution Rayleigh with unit mean, $\alpha=2.2$ [30] is the pathloss exponent. The positions of the PB and the AP are $\{0\,\text{m}, 0\,\text{m}\}$ and $\{0\,\text{m}, 10\,\text{m}\}$ respectively. The users are randomly distributed inside an area with$\{-50\,\text{m}, 50\,\text{m}\}$, $\{-50\,\text{m}, 50\,\text{m}\}$. Several other important siumulation parameters are given in **Table 1**.

In Figures 3-13, we refer our proposed solutions as "TDMA-EH", "TDMA-nonEH", "OFDMA-EH", and "OFDMA-nonEH" for the TDMA-enabled schemes and OFDMA-enabled schemes using a linear EH model and a non-linear EH model, respectively.

As shown in Figure 3, the convergence rate of **Algorithm 1** and **Algorithm 2** is plotted for all schemes. We observed that the proposed algorithms for the TDMA-enabled schemes converge to the maximum SR faster than that for the OFDMA-enabled schemes. Clearly, the SR of the TDMA-enabled WPCNs nearly converges after three iterations, while that of the OFDMA-enabled WPCNs converges after ten iterations. This difference is due to the uncertain values of binary variables on the SC of the OFDMA-enabled WPCNs.

Figure 4 shows the change in the SR in accordance with the transmit power of the PB for various schemes with different

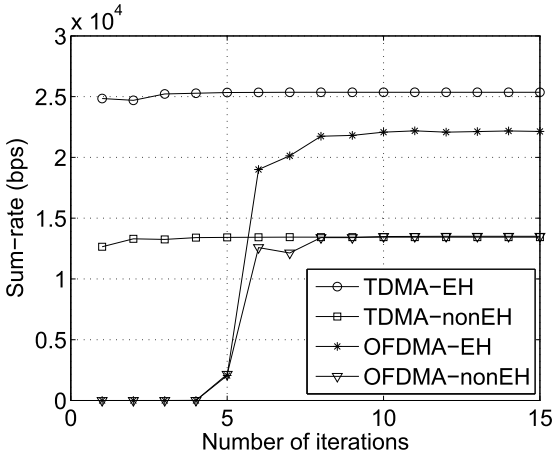

(a) $P_B = 30$ dBm

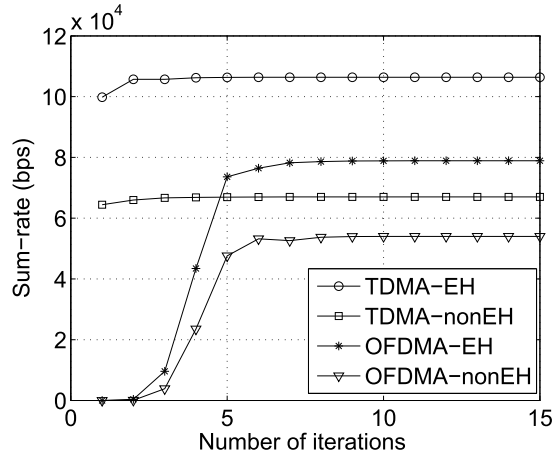

(b) $P_B = 40$ dBm

FIGURE 3. Convergence behavior of the proposed algorithms, $N_T = 4$, $K = 5$, and $d_x = 10$ m.

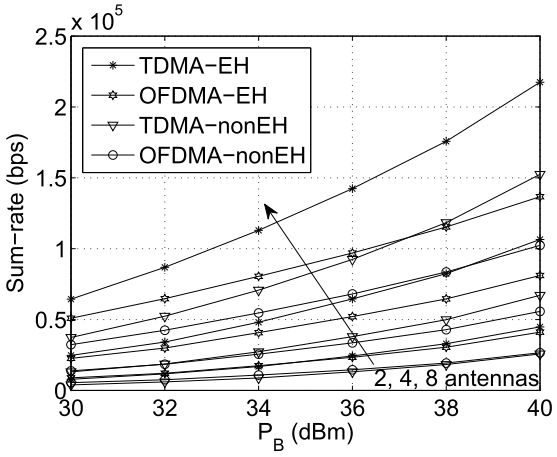

FIGURE 4. Average sum-rate versus the transmit power of the PB for different numbers of antennas at the AP with $K = 5$ and $d_x = 10$ m.

number of antennas at the AP. In this scenario, the distance between the PB and the AP is set as $d_x = 10$ m and the AP serves $K = 5$ IoT users. Figure 4 shows that when the number of antennas at the AP and the transmit power of the PB increase, the SR of all schemes increases. This is

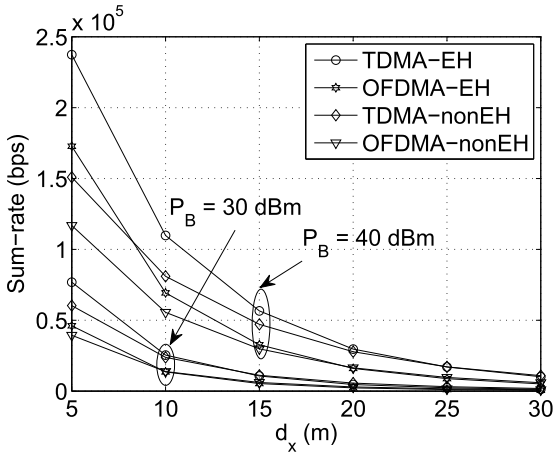

FIGURE 5. Average sum-rate versus the distance between the PB and AP with $N_T = 4$ and $K = 5$.

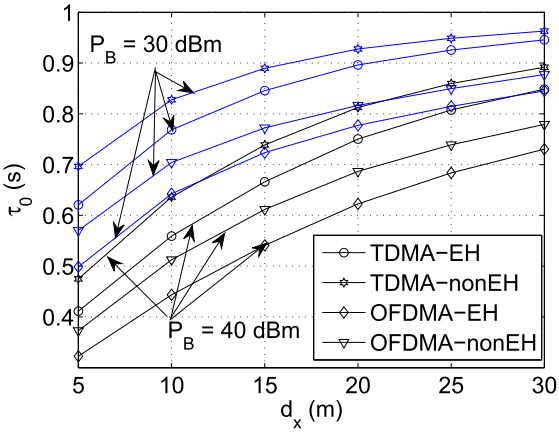

FIGURE 6. EH time versus the distance between the AP and PB with $N_T = 4$ and $K = 5$.

because increase in its number of antennas, the AP harvests more energy, resulting in an improvement in the transmission information quality. In addition, all schemes that adopted TDMA technique are more effective than those that adopted the OFDMA technique and the performance gap between the TDMA-enabled schemes and OFDMA-enabled schemes increases as the number of antennas at the AP increases. The performance of the schemes deploying the non-liear EH model is worst than that of the schemes deploying the linear EH model owing to the limitations of EH circuits in the non-linear EH model.

Figure 5 illustrates the SR as a function of the distance between the PB and the AP when transmit power of the PB are set $P_B = 30$ dBm and $P_B = 40$ dBm. It is observed that the SR descreases significiantly as this distance increases. This means that the greater is the distance between the AP and the PB, the longer is the EH duration of the AP as shown in Figure 6. Correspondingly, there is less time for information transmission from the AP to multiple users, thus the SR reduces. In addition, as the distance increases, the path loss becomes the dominant factor leading to a lower amount of energy received at the AP. The advantage of the schemes

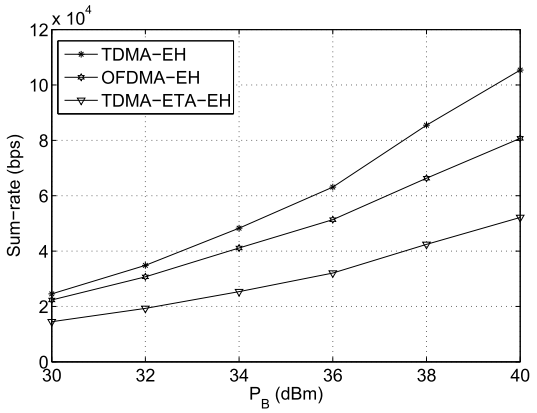

(a) Linear EH models

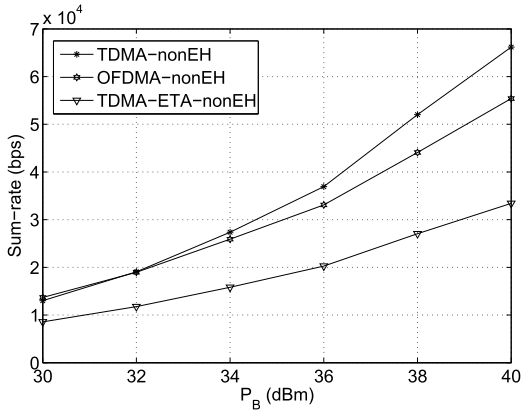

(b) Non-linear EH models

FIGURE 7. Performance comparison between the proposed algorithms and the equal time allocation (ETA) algorithm [16], [17] with $N_T = 4$, $K = 5$ and $d_x = 10$ m.

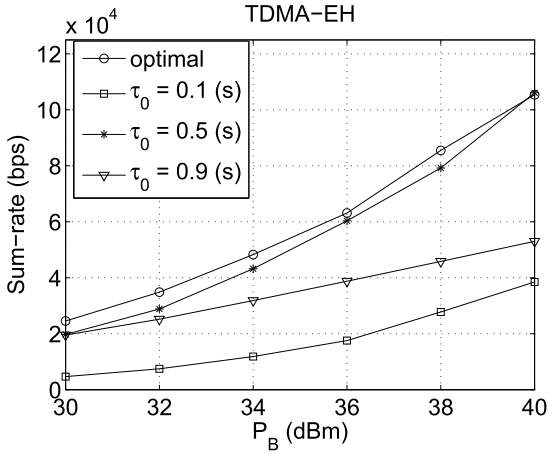

(a) TDMA-EH-enabled schemes

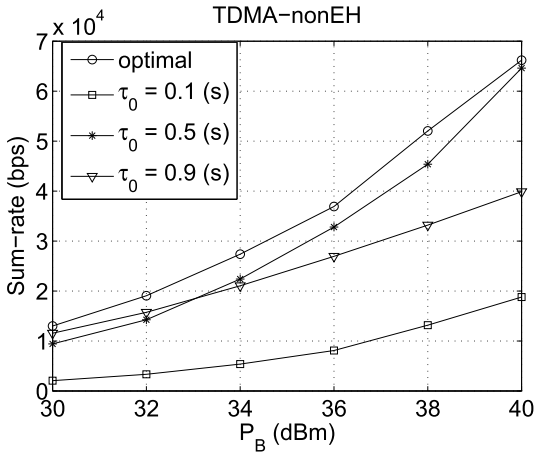

(b) TDMA-nonEH-enabled schemes

FIGURE 8. Performance comparison between the proposed algorithms and the fixed EH time-based algorithm [14], [15] (i.e., $\tau_0 = 0.1(s)$, $\tau_0 = 0.5(s)$, $\tau_0 = 0.9(s)$) with $N_T = 4$, $K = 5$ and $d_x = 10$ m.

using the linear EH model is lost as the AP is placed farther away from the PB. In addition, the duration of EH of the TDMA-enabled schemes is always greater than that of the OFDMA-enabled schemes as shown in Figure 6.

In Figure 7, we compare the performance of the proposed algorithms with that of the ETA algorithm studied in [16], [17] under the different transmit powers of the PB. For the ETA algorithm, from $\sum_{k=0}^{K} \tau_k = 1$, we have $\tau_k = \frac{1}{K+1}, \forall k \in \mathcal{K}$, while the power allocation is similar to that of the TPA algorithm. As can be seen that the performance of the proposed algorithms outperforms that of the ETA algorithm for all schemes. This higher performance is because some users in the ETA algorithm may be allocated insufficient time to communicate with the AP, leading to a strictly suboptimal solution. This phenomenon further confirms the effectiveness of jointly optimizing τ_k and p_k in the considered system.

Figures 8 and 9 compare the performance of the proposed optimal algorithms with the fixed EH time (FEHT) algorithm with different values of τ_0 [14], [15]. For the FEHT algorithm, we only fix the EH duration τ_0 but use the same method for TPA at the AP, similar to the proposed optimal algorithms. As expected, from Figure 8, the proposed optimal algorithms outperform the FEHT for the TDMA-enabled schemes because of the use of optimal jointing time and TPA at the AP. These results verify the effectiveness of our proposed optimal solutions.

However, from Figure 9, the performance of the FEHT-based OFDMA-enabled schemes with $\tau_0 = 0.5$ is close to that of the proposed OFDMA-enabled schemes, using both the linear EH model and non-linear EH model.

From Figure 10, we can see that τ_0 of the proposed OFDMA-enabled schemes is approximately $0.5(s)$; hence, the proposed OFDMA-enabled schemes and FEHT-based OFDMA-enabled schemes exhibit similar performances for $\tau_0 = 0.5(s)$.

The affect of the number of users on the SR of all schemes for $P_B = 30$ dBm and $P_B = 40$ dBm at the PB and two cases of the number of antennas at the AP, i.e., $N_T = 2$, $N_T = 4$ is illustrated in Figure 11, respectively. We can observe that the all schemes tend to reach their maximum SRs when the number of users is more than 2. Specially, the OFDMA-enabled schemes outperform the TDMA-enabled ones when

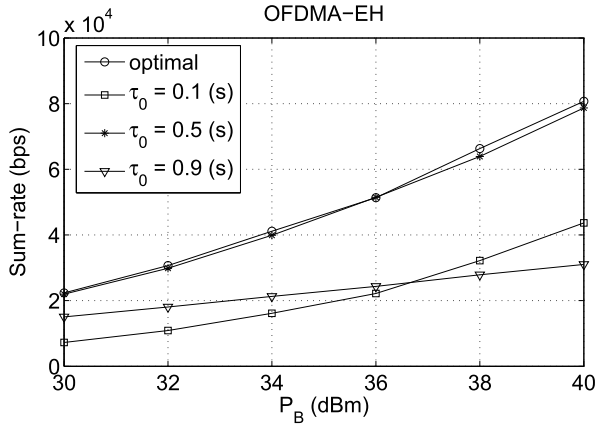

(a) OFDMA-EH-enabled schemes

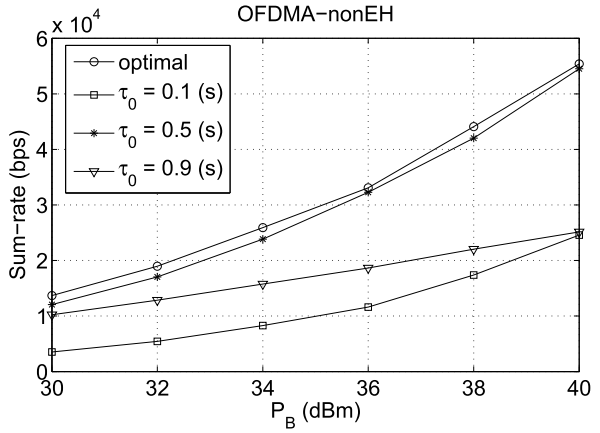

(b) OFDMA-nonEH-enabled schemes

FIGURE 9. Performance comparison between the proposed algorithms and the fixed EH time-based algorithm [14], [15] (i.e., $\tau_0 = 0.1(s)$, $\tau_0 = 0.5(s)$, $\tau_0 = 0.9(s)$), $N_T = 4$, $K = 5$ and $d_x = 10$ m.

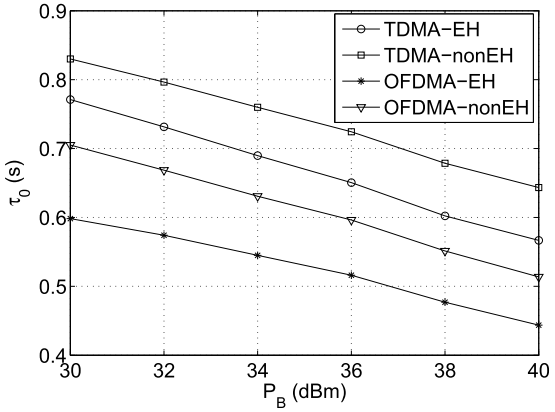

FIGURE 10. EH time versus the transmit power of the PB with $N_T = 4$, $K = 5$ and $d_x = 10$ m.

the number of users increases from 2 to 10 for $N_T = 2$. However, the advantage of OFDMA-enabled schemes compared with that of TDMA-enabled schemes is not significant for $N_T = 4$. The same phenomenon is observed as in the Figure for $N_T = 2$ and $P_B = 40$ dBm. In addition, the TDMA-enabled schemes can harvest more

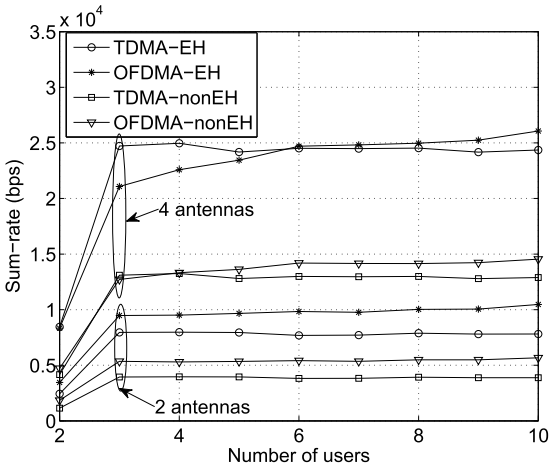

(a) $P_B = 30$ dBm

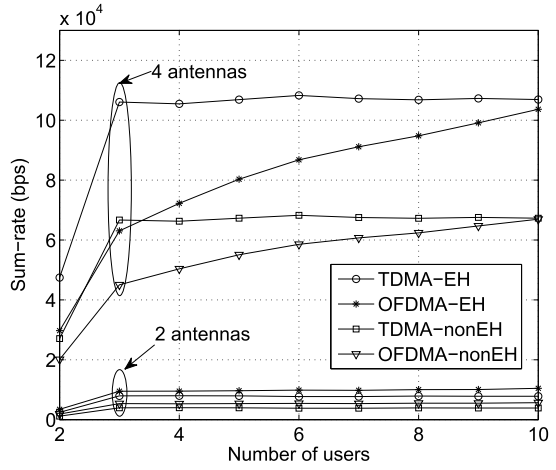

(b) $P_B = 40$ dBm

FIGURE 11. Average sum-rate versus the number of users with (a) $P_B = 30$ dBm, (b) $P_B = 40$ dBm and $d_x = 10$ m.

energy due to taking advantage of having more antennas, i.e., $N_T = 4$, and therefore, their SRs reach saturate values faster than that of the OFDMA-enabled schemes. Moreover, the gap between TDMA-enabled schemes and OFDMA-enabled schemes becomes smaller as the number of users increases for $P_B = 40$ dBm. In the case of the small number of users, the performance of the TDMA-enabled schemes is only better than that of the OFDMA-enabled schemes when the number of antennas at the AP as well as the transmit power at the PB are high enough. In other words, the OFDMA-enabled schemes can be a suitable option when the AP is equipped with a small number of antennas and the transmit power of the PB is also small.

In Figure 12, we evaluate the performance of the schemes that adopt the linear EH model and non-linear EH model as energy conversion efficiency is varied, where $N_T = 4$, $K = 5$, and $d_x = 10$ m. Clearly, the SR of the linear EH-based schemes increases when the energy conversion efficiency varies from 0.1 to 0.9, while that of the non-linear EH-based schemes is constant. In addition, the Figure shows

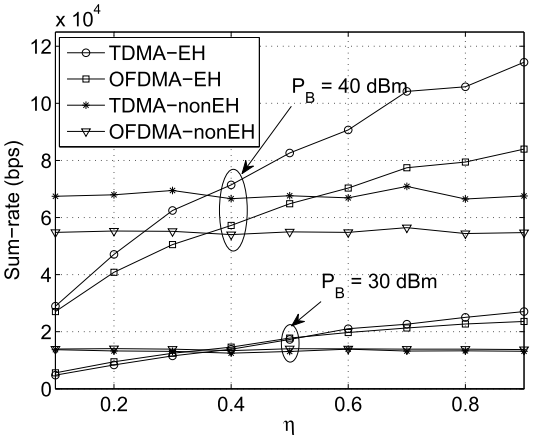

FIGURE 12. Average sum-rate versus the energy conversion efficiency with $N_T = 4$, $K = 5$ and $d_x = 10$ m.

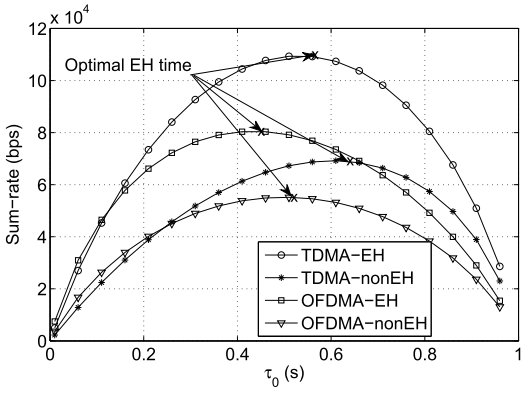

FIGURE 13. Average sum-rate versus the EH time with $N_T = 4$, $K = 5$, $P_B = 40$ dBm and $d_x = 10$ m.

that the performance of the linear EH-based schemes can be equivalent to that of the non-linear EH-based schemes as energy conversion efficiency of the EH circuit is between 0.3 and 0.4.

Figure 13 depicts the SR as a function of EH duration τ_0 for the considered resource allocation schemes. From the Figure, one can observe that the SR function is a concave function with respect to τ_0. This further confirms that we can use 1-D line search, e.g., golden search, to obtain the optimal τ_0^* for all the TDMA-enabled schemes.

VI. CONCLUSION

We studied a WPCN where the AP harvests energy from the PB's RF signals and then employs the harvested energy to convey independent signals to multiple users in the downlink. The SR maximization problem was investigated by optimizing the EH duration and TPA for TDMA and OFDMA, which accounts both linear and non-linear EH circuits. For TDMA-enabled WPCN, we decomposed the original problem into three subproblems which allows us to explicitly exploit the structure of the considered problem. In particular, we obtained the TPA based on the bisection search and the optimal EH time by using a golden section search, and then derived the closed-form of the optimal time allocation for information transmission from the AP to multiple IoT users. For OFDMA-enabled WPCN, by exploiting the quasi-concave form of the problem, we obtained the EH time and the optimal TPA based on bisection search. Numerical results were provided to reveal the effectiveness of the proposed algorithms, compared to the equal time allocation and fixed EH time algorithms for both the non-linear and linear EH models. In addition, we concluded that the SR of the proposed TDMA-enabled WPCN was better than that of the proposed OFDMA-enabled WPCN for a high transmit power of the PB as well as a relatively large number of antennas at the AP. Finally, some potential issues such as maximization of sum rate under IoT user's minimum data rate requirements, beamforming technique for the AP, and determining optimal energy efficiency of the system are crucial for practical systems with a sufficiently large numbers of users served by multiple APs, and thus will be reported in the follow-up work.

APPENDICES

PROOF OF PROPOSITION 1

Now, we introduce the Lagrangian dual function for (P1-2) with a given E_k and τ_0 as

$$L_1(\tau_k, \upsilon) = B\sum_{k=1}^{K}\tau_k \log\left(1+\frac{E_k}{\tau_k}\bar{\gamma}_k\right) - \upsilon\left(\sum_{k=1}^{K}\tau_k - 1 + \tau_0\right), \tag{36}$$

where $\upsilon > 0$ is the Lagrangian multiplier associated with the constraint $\bar{C}_2$ in (P1-2). We take the derivative $L_1(\tau_k, \upsilon)$ with respect to τ_k and set it to zero, i.e., $\partial L_1/\partial\tau_k = 0$ for each k, $1 \le k \le K$. We have

$$\log\left(1+\frac{E_k}{\tau_k}\bar{\gamma}_k\right) - \frac{\frac{E_k}{\tau_k}\bar{\gamma}_k}{1+\frac{E_k}{\tau_k}\bar{\gamma}_k} = \upsilon/B. \tag{37}$$

To satisfy K equations in (37), the following condition exists [6], [29]

$$\frac{E_1}{\tau_1}\bar{\gamma}_1 = \ldots = \frac{E_K}{\tau_K}\bar{\gamma}_K. \tag{38}$$

By denoting $(1/\zeta) = \frac{E_k}{\tau_k}\bar{\gamma}_k$, we obtain

$$\tau_k = \zeta E_k \bar{\gamma}_k. \tag{39}$$

Substituting (39) into $\bar{C}_2$ in (P1-2), we can obtain

$$\zeta\sum_{k=1}^{K}E_k\bar{\gamma}_k = 1-\tau_0, \tag{40}$$

$$\zeta = \frac{1-\tau_0}{\sum_{k=1}^{K}E_k\bar{\gamma}_k}. \tag{41}$$

From (41) and (39), the optimal τ_k^* is determined as in (14).

PROOF OF PROPOSITION 2

The problem of (P1-4) can be rewritten as

$$\max_{\{E_k\}} B(1-\bar{\tau})\sum_{k=1}^{K}\log\left(1+\sum_{k=1}^{K}E_k\left(\frac{\bar{\gamma}_k}{1-\bar{\tau}}\right)\right)$$
$$\text{s.t. } \tilde{C}_3: \sum_{k=1}^{K}E_k \le E_\Theta\bar{\tau},$$
$$\bar{C}_4: 0 \le E_k, \quad \forall k \in \mathcal{K}. \tag{42}$$

For a given $\bar{\tau}$, problem (42) can be easily verified to be a convex problem that satisfies the Slater's condition. Hence, we can apply the Lagrangian duality method to solve the problem.

The Lagrangian function of the problem is given as

$$L(\{E_k\},\chi) = B(1-\bar{\tau})\sum_{k=1}^{K}\log\left(1+\sum_{k=1}^{K}E_k\left(\frac{\bar{\gamma}_k}{1-\bar{\tau}}\right)\right) - \chi\left(\sum_{k=1}^{K}E_k - E_\Theta\bar{\tau}\right), \tag{43}$$

where $\chi \ge 0$ is the Lagrangian multiplier associated with $\tilde{C}_3$. Taking the partial derivative of $L(\{E_k\},\chi)$ with respect to E_k, yields

$$\frac{\partial L(\{E_k\},\chi)}{\partial E_k} = \frac{(1-\bar{\tau})B\left(\frac{\bar{\gamma}_k}{1-\bar{\tau}}\right)}{1+E_k\left(\frac{\bar{\gamma}_k}{1-\bar{\tau}}\right)+\sum_{i=1,i\neq k}^{K}E_i\left(\frac{\bar{\gamma}_i}{1-\bar{\tau}}\right)} - \chi, \tag{44}$$

By solving $\frac{\partial L(\{E_k\},\chi)}{\partial E_k} = 0$, we can obtain the equation given in (17).

REFERENCES

[1] J. An, K. Yang, J. Wu, N. Ye, S. Guo, and Z. Liao, "Achieving sustainable ultra-dense heterogeneous networks for 5G," *IEEE Commun. Mag.*, vol. 55, no. 12, pp. 84–90, Dec. 2017.

[2] S. Vashi, J. Ram, J. Modi, S. Verma, and C. Prakash, "Internet of Things (IoT): A vision, architectural elements, and security issues," in *Proc. Int. Conf. I-SMAC (IoT Social, Mobile, Anal. Cloud) (I-SMAC)*, Feb. 2017, pp. 492–496.

[3] P. Ramezani and A. Jamalipour, "Toward the evolution of wireless powered communication networks for the future Internet of Things," *IEEE Netw.*, vol. 31, no. 6, pp. 62–69, Nov./Dec. 2017.

[4] X. Gao, P. Wang, D. Niyato, K. Yang, and J. An, "Auction-based time scheduling for backscatter-aided RF-powered cognitive radio networks," *IEEE Trans. Wireless Commun.*, vol. 18, no. 3, pp. 1684–1697, Mar. 2019.

[5] K. W. Choi, P. A. Rosyady, L. Ginting, A. A. Aziz, D. Setiawan, and D. I. Kim, "Theory and experiment for wireless-powered sensor networks: How to keep sensors alive," *IEEE Trans. Wireless Commun.*, vol. 17, no. 1, pp. 430–444, Jan. 2018.

[6] Z. Chu, F. Zhou, Z. Zhu, R. Q. Hu, and P. Xiao, "Wireless powered sensor networks for Internet of Things: Maximum throughput and optimal power allocation," *IEEE Internet Things J.*, vol. 5, no. 1, pp. 310–321, Feb. 2018.

[7] R. Zhang and C. K. Ho, "MIMO broadcasting for simultaneous wireless information and power transfer," *IEEE Trans. Wireless Commun.*, vol. 12, no. 5, pp. 1989–2001, May 2013.

[8] D. Sui, F. Hu, W. Zhou, M. Shao, and M. Chen, "Relay selection for radio frequency energy-harvesting wireless body area network with buffer," *IEEE Internet Things J.*, vol. 5, no. 2, pp. 1100–1107, Apr. 2018.

[9] R. Rajesh, V. Sharma, and P. Viswanath, "Capacity of Gaussian channels with energy harvesting and processing cost," *IEEE Trans. Inf. Theory*, vol. 60, no. 5, pp. 2563–2575, May 2014.

[10] X. Wang, Z. Nan, and T. Chen, "Optimal MIMO broadcasting for energy harvesting transmitter with non-ideal circuit power consumption," *IEEE Trans. Wireless Commun.*, vol. 14, no. 5, pp. 2500–2512, May 2015.

[11] W. Lu, Y. Gong, J. Wu, H. Peng, and J. Hua, "Simultaneous wireless information and power transfer based on joint subcarrier and power allocation in OFDM systems," *IEEE Access*, vol. 5, pp. 2763–2770, 2017.

[12] I. Krikidis, S. Timotheou, S. Nikolaou, G. Zheng, D. W. K. Ng, and R. Schober, "Simultaneous wireless information and power transfer in modern communication systems," *IEEE Commun. Mag.*, vol. 52, no. 11, pp. 104–110, Nov. 2014.

[13] T. N. Do, D. B. da Costa, T. Q. Duong, and B. An, "Improving the performance of cell-edge users in MISO-NOMA systems using TAS and SWIPT-based cooperative transmissions," *IEEE Trans. Green Commun. Netw.*, vol. 2, no. 1, pp. 49–62, Mar. 2018.

[14] G. Huang, Q. Zhang, and J. Qin, "Joint time switching and power allocation for multicarrier decode-and-forward relay networks with SWIPT," *IEEE Signal Process. Lett.*, vol. 22, no. 12, pp. 2284–2288, Dec. 2015.

[15] G. Huang, D. Tang, S. Zhao, and J. Qin, "Optimal simultaneous wireless information and energy transfer in OFDMA decode-and-forward relay networks," *Wireless Netw*, vol. 23, no. 6, pp. 1731–1742, Aug. 2017. doi: 10.1007/s11276-016-1249-4.

[16] H. Ju and R. Zhang, "Throughput maximization in wireless powered communication networks," *IEEE Trans. Wireless Commun.*, vol. 13, no. 1, pp. 418–428, Jan. 2014.

[17] D. Xu and Q. Li, "Joint power control and time allocation for wireless powered underlay cognitive radio networks," *IEEE Wireless Commun. Lett.*, vol. 6, no. 3, pp. 294–297, Jun. 2017.

[18] H. Kim, H. Lee, M. Ahn, H.-B. Kong, and I. Lee, "Joint subcarrier and power allocation methods in full duplex wireless powered communication networks for OFDM systems," *IEEE Trans. Wireless Commun.*, vol. 15, no. 7, pp. 4745–4753, Jul. 2016.

[19] X. Zhou, J. Guo, S. Durrani, and M. Di Renzo, "Power beacon-assisted millimeter wave ad hoc networks," *IEEE Trans. Commun.*, vol. 66, no. 2, pp. 830–844, Feb. 2018.

[20] K. Yang, N. Yang, N. Ye, M. Jia, Z. Gao, and R. Fan, "Non-orthogonal multiple access: Achieving sustainable future radio access," *IEEE Commun. Mag.*, vol. 57, no. 2, pp. 116–121, Feb. 2019.

[21] T.-N. Do, V.-D. Nguyen, O.-S. Shin, and B. An, "Simultaneous uplink and downlink transmissions for wireless powered communication networks," *IEEE Commun. Lett.*, vol. 23, no. 2, pp. 374–377, Feb. 2019.

[22] V.-D. Nguyen, T. Q. Duong, H. D. Tuan, O.-S. Shin, and H. V. Poor, "Spectral and energy efficiencies in full-duplex wireless information and power transfer," *IEEE Trans. Commun.*, vol. 65, no. 5, pp. 2220–2233, May 2017.

[23] C.-H. Lee, "Wireless information and power transfer for communication recovery in disaster areas," in *Proc. IEEE Int. Symp. World Wireless, Mobile Multimedia Netw.*, Jun. 2014, pp. 1–4.

[24] E. Boshkovska, D. W. K. Ng, N. Zlatanov, and R. Schober, "Practical non-linear energy harvesting model and resource allocation for SWIPT systems," *IEEE Commun. Lett.*, vol. 19, no. 12, pp. 2082–2085, Dec. 2015.

[25] J. Chen, Z. Zhang, Y.-C. Liang, X. Kang, and R. Zhang, "Resource allocation for wireless-powered IoT networks with short packet communication," *IEEE Trans. Wireless Commun.*, vol. 18, no. 2, pp. 1447–1461, Feb. 2019.

[26] Y. Wang, Y. Wang, F. Zhou, Y. Wu, and H. Zhou, "Resource allocation in wireless powered cognitive radio networks based on a practical non-linear energy harvesting model," *IEEE Access*, vol. 5, pp. 17618–17626, 2017.

[27] P. Ramezani, Y. Zeng, and A. Jamalipour, "Optimal resource allocation for multiuser Internet of Things network with single wireless-powered relay," *IEEE Internet Things J.*, vol. 6, no. 2, pp. 3132–3142, Apr. 2019.

[28] S. Gong, S. Ma, C. Xing, and G. Yang, "Optimal beamforming and time allocation for partially wireless powered sensor networks with downlink SWIPT," *IEEE Trans. Signal Process.*, vol. 67, no. 12, pp. 3197–3212, Jun. 2019.

[29] F. Yang, W. Xu, Z. Zhang, L. Guo, and J. Lin, "Energy efficiency maximization for relay-assisted WPCN: Joint time duration and power allocation," *IEEE Access*, vol. 6, pp. 78297–78307, 2018.

[30] Q. Wu, W. Chen, D. W. K. Ng, and R. Schober, "Spectral and energy-efficient wireless powered IoT networks: NOMA or TDMA?" *IEEE Trans. Veh. Technol.*, vol. 67, no. 7, pp. 6663–6667, Jul. 2018.
[31] Y.-E. Wang, X. Lin, A. Adhikary, A. Grovlen, Y. Sui, Y. Blankenship, J. Bergman, and H. S. Razaghi, "A primer on 3GPP narrowband Internet of Things," *IEEE Commun. Mag.*, vol. 55, no. 3, pp. 117–123, Mar. 2017.

TIEN-TUNG NGUYEN received the B.Sc. and M.Sc. degrees from the University of Science Ho Chi Minh City, Vietnam, in 2005 and 2010, respectively. He is currently pursuing the Ph.D. degree in electronics with Myongji University, South Korea, where he is advised by Prof. Y.-H. Kim. From 2005 to 2010, he worked for Dong Nai Radio Television as a Telecommunication Engineer. Since 2011, he has been a Lecturer of Industrial University of Ho Chi Minh City, HCMC, Vietnam. His research interests include wireless communication and energy harvesting, cognitive radio, NOMA, and machine learning.

VAN-DINH NGUYEN (S'14–M'19) received the B.E. degree in electrical engineering from the Ho Chi Minh City University of Technology, Vietnam, in 2012, and the M.E. and Ph.D. degrees in electronic engineering from Soongsil University, Seoul, South Korea, in 2015 and 2018, respectively. He was a Postdoctoral Researcher and also a Lecturer with the Department of ICMC Convergence Technology, School of Electronic Engineering, Soongsil University, from 2018 to 2019, a Postdoctoral Visiting Scholar with the University of Technology Sydney, Australia, in 2018, and a Ph.D. Visiting Scholar with Queen's University Belfast, U.K., from 2015 to 2016. From 2012 to 2013, he spent 12 months with Vietnam Television as a Principal Engineer. He is currently a Research Associate with the Interdisciplinary Centre for Security, Reliability and Trust (SnT), University of Luxembourg. He has authored or coauthored in some 30 articles published in international journals and conference proceedings. His current research activity is focused on the mathematical modeling of 5G cellular networks and machine learning for wireless communications. He received several best conference paper awards, the IEEE TRANSACTIONS ON COMMUNICATIONS Exemplary Reviewer 2018 and the IEEE GLOBECOM Student Travel Grant Award 2017. He has served as a Reviewer for many top-tier international journals on wireless communications, and has also been a Technical Programme Committee Member for several flag-ship international conferences in the related fields. He is an Editor for the IEEE Open Journal of the Communication Society and IEEE COMMUNICATIONS LETTERS.

JONG-HO LEE (M'13) received the B.S. degree in electrical engineering and the M.S. and Ph.D. degrees in electrical engineering and computer science from Seoul National University, Seoul, South Korea, in 1999, 2001, and 2006, respectively. From 2006 to 2008, he was a Senior Engineer with Samsung Electronics, Suwon, South Korea. From 2008 to 2009, he was a Postdoctoral Researcher with the Georgia Institute of Technology, Atlanta, GA, USA. From 2009 to 2012, he was an Assistant Professor with the Division of Electrical, Electronic, and Control Engineering, Kongju National University, Cheonan, South Korea. From 2012 to 2018, he was an Associate Professor with the Department of Electronic Engineering, Gachon University, Seongnam, South Korea. Since 2018, he has been a Faculty Member with the School of Electronic Engineering, Soongsil University, Seoul. His research interests include wireless communication systems and signal processing for communication with current emphasis on multiple-antenna techniques, multihop relay networks, physical layer security, and full-duplex wireless communications.

YONG-HWA KIM received the B.S. degree in electrical engineering from Seoul National University, Seoul, South Korea, in 2001, and the Ph.D. degree in electrical and computer engineering from Seoul National University, Seoul, in 2007. From 2007 to 2011, he was a Senior Researcher with the Korea Electrotechnology Research Institute (KERI), Geonggi-do, South Korea. From 2011 to 2013, he was an Assistant Professor with the Division of Maritime Electronics and Communication Engineering, Mokpo National Maritime University, South Korea. Since March 2013, he has joined the faculty with the Department of Electronic Engineering, Myongji University, South Korea. His research interests include fault diagnosis for power grids and signal processing for communications with the current emphasis on artificial intelligence, and the Internet-of-Things.